NATIONAAL LUCHT- EN RUIMTEVAARTLABORATORIUM

NATIONAL AEROSPACE LABORATORY NLR

THE NETHERLANDS

NLR MP 78012 U

THE USE OF PANEL METHODS FOR STABILITY DERIVATIVES

BY

R. ROOS

NLR MP 78012 U

THE USE OF PANEL METHODS FOR STABILITY DERIVATIVES

by

R. Roos

Paper presented at AGARD Conference "Dynamic Stability Parameters" held by AGARD Fluid Dynamics Panel, Athens, 22-24 May 1978.

11 pages

Division: Fluid Dynamics
Prepared: RR/ RR 19/5
Approved: HT/ [illegible]

Completed : 7-V-1978
Ordernumber: 108.802
Typ. : GC

THE USE OF PANEL METHODS FOR STABILITY DERIVATIVES*

by
R. Roos
National Aerospace Laboratory, NLR
Amsterdam
The Netherlands

SUMMARY

The possibilities of panel methods for computing aerodynamic stability derivates are reviewed. Emphasis is put on unsteady panel methods, results of which are compared with experimental data.

LIST OF SYMBOLS

A_{ij}	aerodynamic force (eq. A1)
a	speed of sound
C_ℓ	rolling-moment coefficient
C_m	pitching-moment coefficient
C_n	yawing-moment coefficient
C_y	side-force coefficient
C_z	normal-force coefficient
$\bar{c}$	mean chord
F	functional dependence of a singularity distribution
g	density of a singularity distribution
h	displacement
K	wave number (eq. 6)
k	reduced frequency symmetric motions: $k = \omega\ell/U_\infty$; antisymmetric motions: $k = \omega\ell/2U_\infty$
ℓ	reference length
M	Mach number
$\vec{n}$	unit normal
p	roll rate
Q_{ij}	generalized aerodynamic force
q	pitch rate
r	yaw rate
S	shape function
S_w	wing surface area
s	semi span
t	time
U_∞	free stream velocity
u	perturbation in forward velocity
V_n	prescribed normal wash
w	normal wash
x,y,z	Cartesian co-ordinate system
α	angle of attack
β	angle of side slip
β	subsonic: $(1-M_\infty^2)^{1/2}$; supersonic $(M_\infty^2-1)^{1/2}$
γ_o	flight path angle
δ	control surface deflection
ξ,η,ζ	Cartesian co-ordinate system
η	state variable of structural vibration mode
θ	angle of pitch
ρ	density
Φ	velocity potential; mode shape
ϕ	perturbation velocity potential; angle of roll
ψ	angle of yaw
ω	oscillation frequency

Superscripts

'	transformed variable (eq. 4.6)
$\dot{}$	time derivative

Subscripts

e	referring to a aerodynamic co-ordinate axis system
g	referring to a gust
s	referring to a stability co-ordinate axis system
∞	referring to the free stream condition

1. INTRODUCTION

The panel methods referred to in this paper have been developed to determine the potential flow about complex airplane configurations. Their name follows from the fact that the surface of the configuration is divided into a set of small segments, called "panels". Each of these panels is assumed to carry a distribution of so-called singularities, which form elementary solutions of the potential flow equation. By requiring the flow to follow the contour of the particular configuration the density of the singularity distribution on each panel can be found. The combined effect of all singularities results in a description of the sought flow field.

In this paper it is explained in what way panel methods can be instrumental in evaluating the aerodynamic input for investigations on aircraft dynamics. This aerodynamic input is required in the form of aerodynamic derivatives such as stability derivatives, control surface derivatives and gust derivatives. The use of panel methods to compute these derivatives is not new. For example, already in 1969 one finds applications of panel methods for computing stability derivatives (Refs 1,2).

The potentialities of panel methods are clear. In the design phase of an airplane it is necessary to know how changes in the configuration will affect the stability characteristics. While for such studies wind tunnel experiments are prohibitively expensive, the flexibility of panel methods allows for parameter studies at relatively low costs. Further, for configurations like the wide-body transports, the SST or for aircraft equipped with multiple stores, the traditional methods to estimate the derivatives (aerodynamic strip theory or data sheets) have become marginal in their applicability. Here also, panel methods can be extremely useful.

Next to this, it becomes more and more necessary to account for the effects of structural deformations. The introduction of large transport planes and higher flight speeds has set off a trend towards increased structural flexibility, which cannot always be ignored in flight dynamic investigations. Similarly the increased application of flight control systems in modern military aircraft may lead to adverse effects due to coupling with structural deformations. This increased importance of the structural deformations results in an aerodynamic coupling of the rigid body motions and the structural motions, making a time dependent or frequency dependent analysis of the stability derivatives necessary. In this respect it is important to recognize the existence of unsteady (harmonic) panel methods, used in aeroelastic investigations.

* This investigation was carried out under contract for the Scientific Research Branch, Air Materiel Directorate, Royal Netherlands Air Force, (RNLAF).

In the following it is tried to give some insight how panel methods may be used for computing aerodynamic derivatives. First the basics of both steady and unsteady panel methods are touched upon. Next some observations are made as to the possibilities of the different methods. Finally some comparisons are made between calculated and measured stability derivatives. Here emphasis is put upon the use of unsteady panel methods, which introduce the possibility to compute "dynamic" stability derivatives. The material presented in this paper is based partly on reference 3.

2. PANEL METHODS

2.1. Fundamentals

The starting point for the description of the compressible flow field about an aircraft configuration, as applied in panel methods, is the assumption of irrotational, (inviscid), flow. This makes it possible to introduce a velocity potential $\Phi = U_\infty x + \phi$, in which U_∞ is the freestream velocity and ϕ a perturbation potential. After linearization this perturbation potential satisfies the equation

$$(1-M_\infty^2)\,\phi_{xx} + \phi_{yy} + \phi_{zz} - \frac{1}{a_\infty^2}\phi_{tt} - 2\frac{M_\infty}{a_\infty}\phi_{xt} = 0 \qquad (1)$$

and is subject to the boundary condition

$$\frac{\partial S}{\partial t} + (\vec{U}_\infty + \vec{\nabla}\phi).\vec{\nabla}S = 0 \;, \qquad (2)$$

which states that at all times the flow should be tangential to the surface of the configuration, described by the shape function $S(x,y,z,t) = 0$.

For incompressible flow equation (1) reduces to the well known Laplace equation

$$\phi_{xx} + \phi_{yy} + \phi_{zz} = 0 \qquad (3)$$

which then in addition holds for the full potential Φ. In the case of steady compressible flow the Göthert co-ordinate transformation

$$x' = x \;,\; y' = \beta y \;,\; z' = \beta z \qquad (4)$$

transforms for subsonic conditions equation (1) into a Laplace equation, while for supersonic conditions the wave equation

$$\phi_{x'x'} - \phi_{y'y'} - \phi_{z'z'} = 0 \qquad (5)$$

is obtained. In many unsteady flow applications the perturbation potential ϕ can be assumed to have a harmonic behaviour: $\phi = \phi_1 e^{i\omega t}$. Here the Göthert transformation combined with the substitution

$$\phi' = \phi_1\, e^{-iKM_\infty x} \;,\; K = \frac{\omega}{a_\infty \beta^2} \qquad (6)$$

results in a Helmholtz equation

$$\phi'_{x'x'} \pm \phi'_{y'y'} \pm \phi'_{z'z'} + K^2\phi' = 0 \qquad (7)$$

In all types of panel methods the solutions of the Laplace, Helmholtz or Wave equation are found by a linear superposition of fundamental solutions of these equations. For this purpose in general the "source", "doublet" and "vorticity" distributions are used. For the source and doublet distributions the general solutions for the equations then are found as an integral over the weighted distributions placed on the surface of the configuration and the wake:

$$\phi(x',y',z',K) = \iint_{S(\xi',\eta',\zeta')} g(\xi',\eta',\zeta')\; F(x'-\xi',y'-\eta',z'-\zeta',K)\; dS \qquad (8)$$

in which the fundamental solution F depends on the type of distribution used. A general solution for the velocity field is easily found by differentiation. When using a vorticity distribution a similar surface integration gives immediately the general solution for the velocity field. In all cases the weighting function g indicates the still unknown density of a particular distribution.

After having applied the reverse of the transformations defined by (4) and (6), the general solution for the velocity field can be substituted in equation (2), thus effecting the tangential flow condition. This results in an integral equation for the normal wash:

$$\frac{\partial}{\partial n}\iint_{S(\xi,\eta,\zeta)} g(\xi,\eta,\zeta,\omega)\; F(x,y,z,\omega)\; dS = V_n(x,y,z,\omega) \qquad (9)$$

from which the unknown density g can be solved.

In panel methods the surface, of the configuration, is divided in individual elements, called panels. On the panels the source, doublet or vorticity density are taken to vary in a certain way: the earlier methods, such as the source panel method of Hess and Smith (Ref. 4), use a constant density over each panel; the newer methods use higher order functions to approximate the variation of the density per panel, with at the same time enforcing some continuity condition on the panel edges.

This division in panels reduces the integral equation to a system of linear algebraic equations. The unknowns are the coefficients in the approximations for the distributions per panel. The right-hand side of each equation contains the specified normal velocity in one or more points per panel (depending on the number of unknowns). Substitution of the coefficients in the pertinent formulae, results in values for the velocity and pressure distribution along the surface of the configuration.

For a more detailed description of the fundamentals the reader is referred to references 5 and 6.

2.2. Types of panel methods

Over the years several kinds of panel methods have been devised. The major difference lies in the type of fundamental singularity or combination of singularities used. In the following only a few of them are mentioned.

As far as steady methods are concerned, the Vortex-lattice (VL) method is perhaps the first and most simple panel method ever developed. The original idea of Falkner (Ref. 7) was implemented on the computer a.o. by Hedman (Ref. 8). The wing, which is regarded as infinitely thin, is covered with a network of horseshoe-vortices, with their trailing legs extending downstream to infinity and composing the wake. This method is capable of treating lifting surfaces, but due to its neglect of thickness it can not handle complete configurations.

The first method to describe the potential flow about thick bodies was the method of Hess and Smith (Ref. 3), who employed constant source panels. A source distribution is not capable of describing a wake in which the vorticity, shed from a lifting configuration, is carried off to infinity. Therefore this method is limited to non-lifting configurations.

The earlier methods for thick lifting configurations used a combination of two types of distributions: a source distribution on the surface of the configuration and a vorticity or doublet distribution on the wake surface and on the internal camber surface. This scheme forms the basis for methods developed a.o. at Boeing (Ref. 9), Douglas (Ref. 10), NLR (Ref. 11), BAC (Ref. 12) and MBB (Ref. 13). Clearly other set-ups are possible to describe this type of flows, such as a doublet or vorticity distribution on both the surface of the configuration and the wake surface. Lately a trend is developing towards methods with higher order distributions.

The most popular panel method for unsteady flow is the Doublet-lattice (DL) method. This method originally developed by Albano and Rodden (Ref. 14) can be regarded as the unsteady version of the Vortex-lattice method. It describes the unsteady flow field about an infinity thin, harmonically oscillating lifting surface configuration. The singularity used is the pressure doublet, which through chordwise integration over a panel reduces to an unsteady lifting line formulation equivalent to the horseshoe-vortex approach.

Based on the Doublet-lattice formulation several attemps were made to incorporate also the effects of the fuselage and stores into the description of the unsteady flow field. First Kalman, Rodden and Giesing (Ref. 15) computed oscillatory wing/body interference by panelling the body as a ring wing. Later a slender body formulation was added to be able to calculate the unsteady forces on the bodies also (Ref. 16).

At the NLR, the Doublet-lattice method was combined with an unsteady source panel method (Ref. 17). In this (NLRI) method the surfaces of the bodies are covered with panels containing a harmonically oscillating constant source distribution, for which the basic formulation was developed earlier by Hess (Ref. 18). The thickness of the lifting surfaces is still neglected.

Finally Morino (Ref. 19) has developed an unsteady panel method in which source and dipole distributions are placed on the surfaces of both the bodies and the lifting elements of the configuration.

3. POSSIBILITIES FOR CALCULATING STABILITY DERIVATIVES

When considering the use of panel methods to compute aerodynamic derivatives necessary for flight dynamic investigations it is useful first to examine the possibilities of such methods more closely. In doing so, certain derivatives can be excluded beforehand, since the assumptions inherent to panel methods make it impossible to compute them with sufficient accuracy. Further a preliminary choice as to the type of panel method most suitable for computing a particular derivative may be made.

3.1. Limitations due to the neglect of viscosity

Common to all panel methods is the assumption of potential flow, implying the neglect of viscosity. This means that the viscous boundary layer along the surface of the configuration is taken to be non-existing. For the high Reynolds number condition encountered with aircraft, this approximation is acceptable when computing coefficients depending on lift. But for estimates on the drag a modelling of viscous effects is indispensable. Some attempts have been made to combine a panel method approach with a 3D-boundary layer calculation, however, such methods are not yet available for routine computations.

This neglect of the boundary layer has several consequences. Some of the derivatives used in stability investigations depend very much on the drag experienced by the aircraft. This drag is built up of viscous drag and induced drag, while for flows with shock waves the wave drag may give an appreciable contribution also. It is clear that this type of derivatives cannot be computed with panel methods in which the boundary layer is not modelled. One possible exception should be mentioned. When the drag derivatives depend mainly on the induced drag, being a function of the lift coefficient, a reasonable estimate might be obtained.

Further the forces experienced by control surfaces depend strongly on the boundary layer also. Therefore panel methods do not seem very promising for predicting control surface derivatives. On the other hand it is possible that although no accurate values may be obtained, trends may be predicted reasonably well, provided that no flow separation occurs.

This introduces an additional serious limitation of the neglect of viscosity namely that flow separation cannot be modelled. A possible exception is the case of leading edge separation, as occurring for delta wings at high angles of attack, where recently some progress was made. Here the assumption of potential flow could be retained by assuming a vortex sheet to be shed from the leading edge and to roll up into a core of concentrated vorticity. Typical examples of panel methods following this approach are presented in references 20 and 21.

3.2. Modelling of compressibility

The assumption of a perturbation potential and the linearization, makes it impossible to treat transonic flow conditions with panel methods based on equation (1). In addition the results of such methods will have a Mach number dependence following the $(1-M_\infty^2)$ behaviour of the Göthert rule, which is acceptable up to moderately subsonic flow. For high subsonic flow conditions compressibility corrections such as the one devised at NLR (Ref. 3) may be used. In unsteady methods a "local Mach number correction" Ref. (22) may be useful.

Derivatives with respect to the forward velocity are usually expressed in terms of a sum of derivatives with respect to Mach number, dynamic pressure and thrust coefficient. Of these, only derivatives with respect to Mach number can be evaluated with panel methods. This may be done by performing computations for two different Mach numbers and determining the coefficient according to

$$\frac{\partial C}{\partial M} \sim \frac{C(M + \Delta M) - C(M)}{\Delta M} .$$

3.3. Representation of thickness of wings and bodies

For panel methods a clear distinction can be made between planar and non-planar methods. In the planar methods the thickness of the lifting surfaces and the fuselage type parts of the configuration are neglected, while in the fully non-planar methods the thickness of all parts of the configuration is taken into account. A mixture of both is obtained when the lifting surfaces are taken to be thin, while the fuselage is represented correctly. An example of this approach is the NLRI method mentioned in section 2.2

Experience with panel methods has shown that including the wing thickness while neglecting the boundary layer leads to an overestimation of the normal force derivatives on the wing. Due to that the results of planar methods often compare better with experimental data. Clearly, for derivatives to which the fuselage or other thick bodies (such as stores) contribute significantly, non-planar methods or the mixture type methods seem suited most.

In general, applying non-planar methods is more expensive than using planar methods. Therefore, including the effects of fuselage or stores is relatively costly. However, it is possible to introduce the effects of such bodies in an approximate way in planar methods. This is done by representing these bodies in the form of a ring wing, an endplate or a cross. Of course, one has to be careful in applying this type of idealizations, as a certain representation might give good results for one derivative but not for another.

3.4. Application of methods for harmonic motions

The aerodynamic derivatives may be divided in two groups. One group can be computed in principle by a steady method, while the second one can only be evaluated with an unsteady method. In table 1 it is indicated which coefficient belongs to which group. Of course, when making this distinction it should be mentioned that in principle all derivatives can be computed with an unsteady method. The type of unsteady panel methods most commonly in use are those in which small harmonic motions are assumed. In the appendix it is indicated how such methods can be used to obtain the necessary aerodynamic coefficients. In this context it is of interest to mention that all coefficients given in tables A.2 and A.3 can be computed individually. This may be in aid of interpreting results of unsteady windtunnel experiments where many coefficients can be measured only in combination.

TABLE 1

The method of computation of the aerodynamic derivatives depending on their state variable

	Symmetric motions	Antisymmetric motions
Steady method	u, α, q, η δ	β, p, r, η δ
Unsteady method	$\dot\alpha, \dot q, \dot\eta$ $\dot\delta, \dot\alpha_g, \alpha_g$	$\dot\beta, \dot p, \dot r, \dot\eta$ $\dot\delta, \dot\alpha_g, \dot\beta_g, \alpha_g, \beta_g$

3.5. Relation between aircraft motions and input for steady methods

In the stability axis system an α-variation is equivalent to a variation in the constant upwash experienced by the airplane (Fig. 1). Therefore it is equivalent also to the angle of attack variation to be prescribed in the panel methods, where an aerodynamic axis system is used. A variation with respect to q as defined in the stability axis system is felt by the airplane as a linearly varying upwash (see Fig.2). Computation of the corresponding derivatives is possible with steady panel methods when the normal wash is specified individually for each panel.

These observations made for the derivatives with respect to the symmetric variables α and q,are valid also for the derivatives with respect to the anti-symmetric variables β, p and r. However, for the derivatives with respect to β and r the accuracy may become questionable at large yawing angles, when there is a large shadow-effect of the fuselage on the lee side wing and a strong interference of the wake of the weather-side wing with the fuselage (see Fig. 3). The shadow effect depends very much on the development of the boundary layer along the fuselage and therefore is not represented in inviscid panel methods. The direct interference of the wake with the fuselage cannot be represented either, although alignment of the trailing vortices with the free stream direction will account for part of the wake effect.

Derivatives resulting from structural deformation, may be calculated also with steady panel methods by specifying the local normal wash per panel. This normal wash is then derived from a given upwash distribution over the configuration, an example of which is given in figure 4.

4. RESULTS OBTAINED WITH UNSTEADY PANEL METHODS

The applicability of steady panel methods for computing stability derivatives is well documented in the literature. Therefore in this paper the emphasis is put on results obtained with unsteady panel methods, which are hard to find in the literature. As far as planar methods are concerned, Rodden and Giesing (Ref. 24) showed the possibilities of the Doublet-lattice method by computing the longitudinal dynamic stability derivatives for a jet transport wing. Unfortunately no comparison with experimental data was given.

To the authors knowledge the first application of an unsteady non-planar method was reported in reference 22. Using the NLRI-method, discussed in section 2.2, the longitudinal dynamic stability derivatives were computed for a delta wing-fuselage configuration at zero angle of attack. The panelling scheme (for symmetry reasons only one half of the configuration) and the results are given in figure 5. For the few derivatives, obtained in an oscillatory windtunnel experiment (Ref. 25), the theory shows a reasonable agreement.

Recently the NLRI panel method was applied also to calculate the lateral stability derivatives for a T-tail transport configuration. For this configuration experimental data were obtained with the small amplitude forced oscillatory roll mechanism at Nasa Langley (Ref. 26). The panelling scheme used in the calculations is shown in figure 6 (again for symmetry reasons only one half is shown). The fuselage of the configuration was approximated by a blunt nosed cylinder with in contrast to the experimental model, no tapering at the rear. The fuselage mounted engine nacelles were not modelled in the calculations, since in the tests their effect was found to be negligible.

In table 2 a comparison is presented of the calculated and measured derivatives for the configurations with and without wings. For the configuration without the wing the agreement between theory and experiment is reasonably good. The effect of adding the wing is predicted fairly well also, except for the cross derivative C_{n_p}. However, this latter difference can be expected since the main contributions of the wing to this derivative come from profile drag and leading edge suction, which are not modelled in the NLRI-method.

TABLE 2

Comparison of calculated and measured lateral stability derivatives for a T-tail transport

	Fuselage + T-tail		Fuselage + wings + T-tail	
	Theory	Experiment	Theory	Experiment
C_{ℓ_p}	-0.029	-0.025	-0.531	-0.465
$k^2C_{\ell_{\dot{p}}}$	0	0	0	0.004
C_{n_p}	0.052	0.060	0.012	-0.04
$k^2C_{n_{\dot{p}}}$	0	0	0.001	0

Calculations were performed also for isolated parts of the configuration such as the fuselage, the wing and the T-tail. The results (table 3) clearly show the effect on the derivatives when the configuration is made more complex by adding T-tail and wings to it. They indicate also that summing up the contributions due to the isolated parts of the configuration in general is not allowed, because of aerodynamic interference. A typical example for this is the C_{y_p} derivative.

To illustrate in more detail the importance of the aerodynamic interference, the individual contributions of the different parts of the configuration to the derivatives have been listed in table 4. Comparison of tables 3 and 4 show that in general the wing itself is less affected by interference. However, the presence of the wing has a marked influence on the body and even more strongly on the T-tail. Clearly the wake of the wing should be taken into account when computing the contribution due to the T-tail.

5. CONCLUDING REMARKS

In the foregoing the use of panel methods for computing stability derivatives has been discussed. Reasons were given why not all derivatives, especially those which are dominated by viscous drag, can be computed with the same level of accuracy.

The unsteady panel methods, developed for aeroelastic applications, were shown to be very useful for computing "dynamic" stability derivatives. With the aid of some computed examples compared with experimental data, the value of such methods was demonstrated. In addition the calculations showed that parameter studies, in which the contribution of different parts of the configuration are evaluated, can be carried out very succesfully with panel methods.

It was further indicated that planar panel methods, which are cheaper to use, in many cases will give satisfactory results.

TABLE 3

Calculated lateral stability derivatives for different parts of a T-tail transport configuration

	Fuselage	Wings	T-tail	Fuselage T-tail	Fuselage wings T-tail
C_{y_β}	-0.052	-0.001	-0.082	-0.200	-0.237
$C_{y_{\dot\beta}}$	-0.133	0	-0.006	-0.105	-0.072
C_{y_p}	0	0.029	0.039	0.060	-0.035
$C_{y_{\dot p}}$	0	0	0.003	-0.011	0.116
C_{y_r}	-0.618	0	-0.191	-0.804	-0.675
$C_{y_{\dot r}}$	20.8	0.020	32.9	80.0	95.0
C_{ℓ_β}	0	0.015	0.030	0.043	0.025
$C_{\ell_{\dot\beta}}$	0	0	-0.001	-0.002	-0.005
C_{ℓ_p}	0	-0.506	-0.027	-0.029	-0.531
$C_{\ell_{\dot p}}$	0	0.010	0	0.007	-0.008
C_{ℓ_r}	0	-0.001	0.058	0.081	0.066
$C_{\ell_{\dot r}}$	0	-3.04	-11.8	-17.1	-9.95
C_{n_β}	0.052	0	-0.071	-0.073	-0.080
$C_{n_{\dot\beta}}$	-0.007	0	-0.006	0.014	0.037
C_{n_p}	0	0	0.035	0.052	0.012
$C_{n_{\dot p}}$	0	0	0.003	-0.008	0.077
C_{n_r}	-0.124	0	-0.169	-0.296	-0.206
$C_{n_{\dot r}}$	-21.0	0	28.4	28.9	31.9

TABLE 4

Contributions of the different parts of the configuration to the calculated lateral stability derivatives

	Fuselage	Wings	Stabilizer	Fin	Fuselage wings stabilizer fin
C_{y_β}	-0.115	0.003	0	-0.126	-0.237
$C_{y_{\dot\beta}}$	-0.077	0	0	0.005	-0.072
C_{y_p}	-0.065	0.031	0	-0.001	-0.035
$C_{y_{\dot p}}$	0.068	-0.001	0	0.049	0.116
C_{y_r}	-0.463	0.001	0	-0.232	-0.675
$C_{y_{\dot r}}$	46.0	-1.162	0	50.2	95.0
C_{ℓ_β}	0	-0.023	0.017	0.030	0.025
$C_{\ell_{\dot\beta}}$	0	0.002	-0.006	-0.001	-0.005
C_{ℓ_p}	0	-0.523	-0.008	0	-0.531
$C_{\ell_{\dot p}}$	0	0.016	-0.012	-0.012	-0.008
C_{ℓ_r}	0	0.007	0.008	0.051	0.066
$C_{\ell_{\dot r}}$	0	9.2	-6.9	-12.2	-9.95
C_{n_β}	0.029	0	0	-0.109	-0.080
$C_{n_{\dot\beta}}$	0.034	0	0	0.003	0.037
C_{n_p}	0.010	0.001	0	0	0.012
$C_{n_{\dot p}}$	0.034	0	0	0.043	0.077
C_{n_r}	-0.016	0	0	-0.190	-0.206
$C_{n_{\dot r}}$	-11.8	0.129	0	43.5	31.9

6. REFERENCES

1 Dusto, A.R., Chevalier, H.C., Dornfeld, G.M. and Schwanz, R.C.: An analytical method for predicting the stability and control characteristics of large elastic airplanes at subsonic and supersonic speeds. Part I and II. AGARD Conf. Proc. 46, 1969.

2 Roskam, J.: Comments, interpretation and application of a method for predicting aerodynamic characteristics of large flexible airplanes. AGARD Conf. Proc. 46, 1969.

3 Labrujère, Th.E., Roos, R. and Erkelens, L.J.J.: The use of panel methods with a view to problems in aircraft dynamics. VKI lecture series 99, 1977. Also NLR MP 77009 U.

4 Hess, J.L. and Smith, A.M.O.: Calculation of potential flow about arbitrary bodies. Progress in Aeronautical Sciences, Vol 8, Pergamon, London 1967, pp 1-138.

5 Labrujère, Th.E.: A survey of current collocation methods in inviscid subsonic lifting surface theory. Part I: Numerical Aspects. VKI Lecture series 44, Febr. 1972.

6 Hunt, B.: The panel method for subsonic aerodynamic flows. VKI Lecture series 1978-4.

7 Falkner, V.M.: The calculation of aerodynamic loading on surfaces of any shape. ARC, R and M 1910, 1943.

8 Hedman, S.G.: Vortex lattice method for calculation of quasi-steady state loadings on thin elastic wings in subsonic flow. FFA report 105, 1966.

9 Rubbert, P.E. et al: A general method for determining the aerodynamic characteristics of fan-in-wing configurations. The Boeing Co Report D6-15047-1, 1967.

10 Hess, J.L.: Calculation of potential flow about arbitrary three-dimensional lifting bodies. Phase I Final report. McDonnell Douglas Rept.No.MDC-J 0545, 1969.

11 Labrujère, Th.E., Loeve, W. and Slooff, J.W.: An approximate method for the calculation of the pressure distribution on wing-body combinations at sub-critical speeds. AGARD C.P. No. 71, paper 11, 1970. Also NLR MP 70014 U.

12 Hunt, B. and Semple, W.G.: The BAC(MAD) program to solve the 3D lifting subsonic Neumann problem using the plane panel method. BAC doc. ARG 97, 1976.

13 Kraus, W.: Das MBB-UFE Unterschall-Panelverfahren. UFE 633-70, 1970.

14 Albano, E. and Rodden, W.P.: A doublet-lattice method for calculating lift distributions on oscillating surfaces in subsonic flow. AIAA. J. Vol.7, No.2, 1969, pp 279-285.

15 Kalman, T.P., Rodden, W.P. and Giesing, J.P.: Application of the Doublet-Lattice method to Non planar configurations in subsonic flow. J. of Aircraft, Vol.8, June 1971, pp 406-413.

16 Rodden, W.P., Giesing, J.P. and Kalman, T.P.: New developments and applications of the subsonic doublet-lattice method for non-planar configurations. Douglas Aircraft Co paper 5826. AGARD Conf. Proc. no.80-71, part II, No.4, 1971.

17 Roos, R., Bennekers, B. and Zwaan, R.J.: Calculation of unsteady subsonic flow about harmonically oscillating wing/body configurations. J. Aircraft, Vol.14, No.5, May 1977, pp 447-454.
18 Hess, J.L.: Calculation of acoustic fields about arbitrary three-dimensional bodies by a method of surface source distributions based on certain wave number expansions. Douglas Aircr. Comp. Long Beach, Calf.,DAC 66901, March 1968.
19 Morino, L.: A general theory of unsteady compressible potential aerodynamics. NASA CR-2464, 1974.
20 Johnson, F.T., Lu, P., Brune, G.W., Weber, W. and Rubbert, P.E.: An improved method for the predictions of completely three-dimensional aerodynamic load distributions of configurations with leading edge vortex separation. AIAA paper 76-417.
21 Kandil, O.A., Mook, D.T. and Nayfeh, A.H.: Nonlinear prediction of the aerodynamic loads on lifting surfaces. J. of Aircraft, Vol.13, No.1, Jan. 1976, pp 27-28.
22 Roos, R.: Application of panel methods for unsteady subsonic flow. NLR MP 76010 U, 1976.
23 Meyer, J.J. and Zwaan, R.J.: Calculations of frequency response functions for flexible aircraft. NLR TR 75147 U, 1975.
24 Rodden, W.P. and Giesing, J.P.: Application of oscillatory aerodynamic theory to estimation of dynamic stability derivatives. J. of Aircraft, Vol.7, No.3, 1970, pp 272-275.
25 Scherer, M.: Mesure des coefficients de stabilité dans les souffleries transoniques et supersoniques de l'ONERA. Communication à la session de l'AGARD à Marseille, Sept. 1959.
26 Boyden, R.P.: Aerodynamic roll damping of a T-tail transport configuration. NASA TM X-3115, 1974.

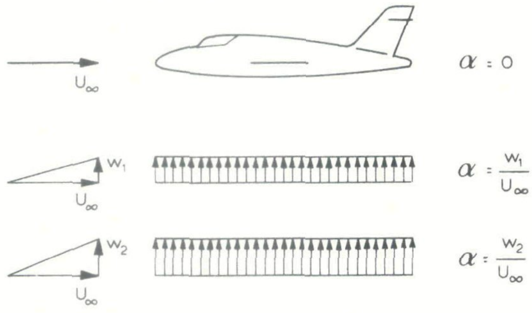

Fig. 1 An α variation in terms of an upwash variation

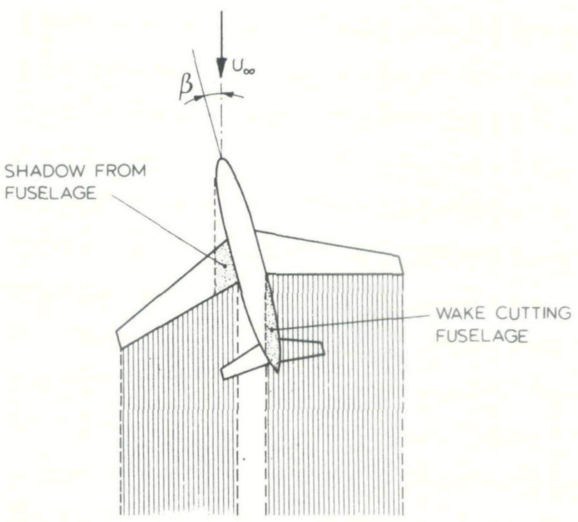

Fig. 3 Poor modelling capabilities for an aircraft subject to a yaw angle

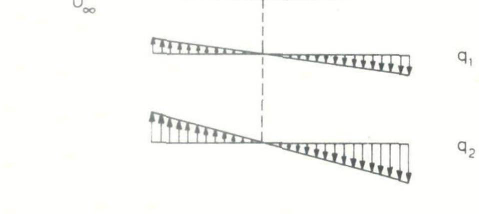

Fig. 2 A q variation in terms of an upwash variation

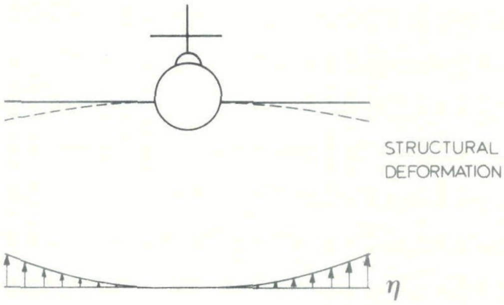

Fig. 4 Example of an upwash distribution for the computation of derivatives with respect to η

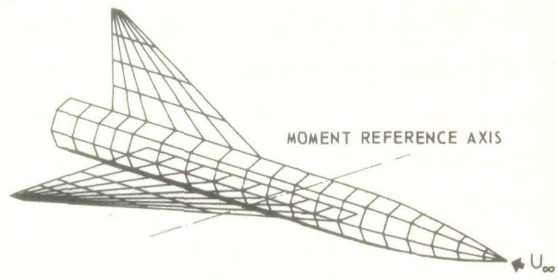

$M_\infty = 0.6$ $k = 0.014$		
	CALCULATED	MEASURED
C_{z_α}	−2.574	−2.510
$C_{z_{\dot\alpha}}$	0.487	
C_{z_q}	−1.211	
C_{m_α}	−0.443	−0.420
$C_{m_{\dot\alpha}}$	0.226	
C_{m_q}	−0.382	−0.315

Fig. 5 Comparison of dynamic stability derivatives as measured in a windtunnel and computed with an unsteady non–planar panel method

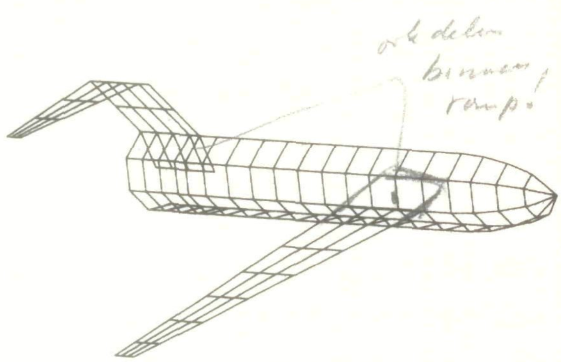

Fig. 6 Panelling scheme for a T – tail transport configuration

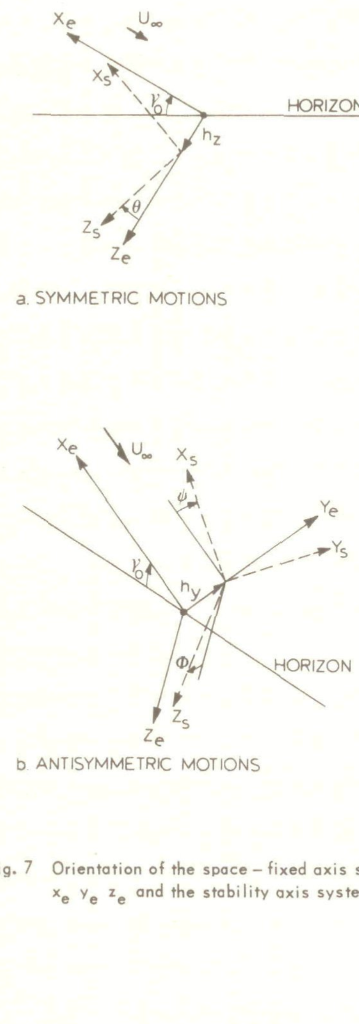

Fig. 7 Orientation of the space – fixed axis system $x_e\ y_e\ z_e$ and the stability axis system $x_s\ y_s\ z_s$

APPENDIX : ANALYTICAL DESCRIPTION OF THE AERODYNAMIC DERIVATIVES

In the stability axis system a typical aerodynamic force is defined as:

$$A_{ij}(t) = \tfrac{1}{2}\rho U_\infty^2 S_W C_{i_{\xi_j}}(t)\, \xi_j(t) \qquad (A.1)$$

in which ξ_j represents a state variable (rigid or flexible), a control surface deflection or gust variable. The index i refers to one of the rigid body motions or one of the structural vibrations. The non-dimensional aerodynamic derivative is defined as:

$$C_{i_{\xi_j}}(t) = \frac{1}{S_W}\iint C_{p_{\xi_j}}(t)\, \vec{n} \cdot \vec{\phi}_i \, dS \qquad (A.2)$$

with $C_{p_{\xi_j}}$ being the change in the local pressure distribution due to a change in the state variable ξ_j. $\vec{\phi}_i$ represents the i^{th} mode shape. For the rigid body motions $\vec{\phi}_i$ takes very simple forms; for symmetric motions e.g.: longitudinal $\vec{\phi}_x = (1,0,0)$, normal $\vec{\phi}_z = (0,0,1)$ and in pitch $\vec{\phi}_m = (\frac{z-z_m}{\bar{c}}, 0, -(\frac{x-x_m}{\bar{c}})$.

The aerodynamic force as defined in (A.1), can be expanded as follows:

$$A_{ij}(t) = \tfrac{1}{2}\rho U_\infty^2 S_W \left[C_{i_{\xi_j}} \xi_j + C_{i_{\dot{\xi}_j}} \dot{\xi}_j + O(\ddot{\xi}) \right] \qquad (A.3)$$

Neglecting the terms involving $\ddot{\xi}$ and higher order derivatives, the aerodynamic force can be regarded as being built up of a steady term and an unsteady term. The derivative $C_{i_{\xi_j}}$ is a quasi-steady quantity and thus can be computed with a steady aerodynamic method (see table 1).

The derivative $C_{i_{\dot{\xi}_j}}$ can be obtained with the existing aerodynamic methods for harmonic aircraft motions, developed for aeroelastic applications. As a rule, the output of these methods comes in the form of generalized aerodynamic forces which refer to an axis system $x_e y_e z_e$ with the x_e-axis pointing in the direction of the undisturbed flight path, while the origin is translating in that direction with a speed U_∞. These generalized aerodynamic forces are defined as a function of the oscillation frequency ω:

$$A_{mn}(\omega) = \tfrac{1}{2}\rho U_\infty^2 s^2 \left[Q'_{mn} + i\, Q''_{mn} \right] \xi_j \qquad (A.4)$$

in which

$$Q_{mn} = \frac{1}{s^2}\iint C_{p_n} \vec{n} \cdot \vec{\phi}_m \, dS \qquad (A.5)$$

As small disturbances have been assumed, simple conversion rules exist between harmonic motions in both the $x_s y_s z_s$ stability axis system and the $x_e y_e z_e$ axis system. For the rigid body motions with a frequency ω these rules are given in table A.1.

TABLE A.1

Conversion rules between the stability and the aerodynamic axis system

	$x_s y_s z_s$ stability system		$x_e y_e z_e$ aerodynamic space-oriented axis system
Symmetric motions	α	=	$ik\frac{h_z}{\bar{c}} + \theta$
	q	=	$ik\theta$
Antisymmetric motions*	β	=	$ik\frac{h_y}{\bar{c}} - \psi$
	p	=	$\tfrac{1}{2} ik\phi$
	r	=	$\tfrac{1}{2} ik\psi$

* The factor ½ in the expressions for p and r enters due to non-dimensionalizing with 2 U_∞ instead of U_∞ as in the case of q.

In this table k is the non-dimensional (reduced) frequency and h_z and h_y are translatory motions in the z_e and y_e directions respectively. The orientation of both axis systems is illustrated in figure 7. The expressions describing the structural vibrations, control surface deflections and atmospheric gusts are the same in both axis systems.

Applying a Fourier transformation the aerodynamic force defined in (A.3) can be written as:

$$A_{ij}(\omega) = \tfrac{1}{2}\rho U_\infty^2 S_W \left[C_{i_{\xi_j}} + ikC_{i_{\dot{\xi}_j}} \right] \xi_j \qquad (A.6)$$

Comparing the expressions (A.4) and (A.6) and using the conversion rules as given in table A.1 relations between the two types of aerodynamic derivatives are derived easily. They are given in tables A.2 and A.3 for the symmetric and antisymmetric derivatives respectively, (taken from ref. 23).

TABLE A.2

Relation between symmetric aerodynamic derivatives and generalized aerodynamic forces

	C_z	C_m	C_{ξ_i}
α	$\frac{s^2}{S_w}\frac{Q''_{22}}{k}$	$\frac{s^2}{S_w}\frac{Q''_{32}}{k}$	$\frac{s^2}{S_w}\frac{Q''_{i2}}{k}$
$\dot{\alpha}$	$-\frac{s^2}{S_w}\frac{Q'_{22}}{k^2}$	$-\frac{s^2}{S_w}\frac{Q'_{32}}{k^2}$	$-\frac{s^2}{S_w}\frac{Q'_{i2}}{k^2}$
q	$\frac{s^2}{S_w}\left(\frac{Q''_{23}}{k}+\frac{Q'_{22}}{k^2}\right)$	$\frac{s^2}{S_w}\left(\frac{Q''_{33}}{k}+\frac{Q'_{32}}{k^2}\right)$	$\frac{s^2}{S_w}\left(\frac{Q''_{i3}}{k}+\frac{Q'_{i2}}{k^2}\right)$
$\dot{q}$	$-\frac{s^2}{S_w}\left(\frac{Q'_{23}}{k^2}-\frac{Q''_{22}}{k^3}\right)$	$-\frac{s^2}{S_w}\left(\frac{Q'_{33}}{k^2}-\frac{Q''_{32}}{k^3}\right)$	$-\frac{s^2}{S_w}\left(\frac{Q'_{i3}}{k^2}-\frac{Q''_{i2}}{k^3}\right)$
ξ_j	$\frac{s^2}{S_w}Q'_{2j}$	$\frac{s^2}{S_w}Q'_{3j}$	$\frac{s^2}{S_w}Q'_{ij}$
$\dot{\xi}_j$	$\frac{s^2}{S_w}\frac{Q''_{2j}}{k}$	$\frac{s^2}{S_w}\frac{Q''_{3j}}{k}$	$\frac{s^2}{S_w}\frac{Q''_{ij}}{k}$
δ	$\frac{s^2}{S_w}Q'_{2\delta}$	$\frac{s^2}{S_w}Q'_{3\delta}$	$\frac{s^2}{S_w}Q'_{i\delta}$
$\dot{\delta}$	$\frac{s^2}{S_w}\frac{Q''_{2\delta}}{k}$	$\frac{s^2}{S_w}\frac{Q''_{3\delta}}{k}$	$\frac{s^2}{S_w}\frac{Q''_{i\delta}}{k}$
α_g	$\frac{s^2}{S_w}Q'_{2\alpha_g}$	$\frac{s^2}{S_w}Q'_{3\alpha_g}$	$\frac{s^2}{S_w}Q'_{i\alpha_g}$
$\dot{\alpha}_g$	$\frac{s^2}{S_w}\frac{Q''_{2\alpha_g}}{k}$	$\frac{s^2}{S_w}\frac{Q''_{3\alpha_g}}{k}$	$\frac{s^2}{S_w}\frac{Q''_{i\alpha_g}}{k}$

Subscripts of Q_{mn} indicate the mode shape:

2 = vertical translation, 3 = pitching motion, i,j = structural vibration, δ = control surface deflection, α_g = gust

TABLE A.3

Relation between antisymmetric aerodynamic derivatives and generalized aerodynamic forces

	C_y	C_ℓ	C_n	C_{ξ_i}
β	$\frac{s^2}{S_w}\frac{Q''_{11}}{k}$	$\frac{s^2}{S_w}\frac{Q''_{21}}{k}$	$\frac{s^2}{S_w}\frac{Q''_{31}}{k}$	$\frac{s^2}{S_w}\frac{Q''_{i1}}{k}$
$\dot{\beta}$	$-\frac{s^2}{S_w}\frac{Q'_{11}}{k^2}$	$-\frac{s^2}{S_w}\frac{Q'_{21}}{k^2}$	$-\frac{s^2}{S_w}\frac{Q'_{31}}{k^2}$	$-\frac{s^2}{S_w}\frac{Q'_{i1}}{k^2}$
p	$\frac{s^2}{S_w}\frac{2Q''_{12}}{k}$	$\frac{s^2}{S_w}\frac{2Q''_{22}}{k}$	$\frac{s^2}{S_w}\frac{2Q''_{32}}{k}$	$\frac{s^2}{S_w}\frac{2Q''_{i2}}{k}$
$\dot{p}$	$-\frac{s^2}{S_w}\frac{2Q'_{12}}{k^2}$	$-\frac{s^2}{S_w}\frac{2Q'_{22}}{k^2}$	$-\frac{s^2}{S_w}\frac{2Q'_{32}}{k^2}$	$-\frac{s^2}{S_w}\frac{2Q'_{i2}}{k^2}$
r	$\frac{s^2}{S_w}\left(\frac{2Q''_{13}}{k}-\frac{2Q'_{11}}{k^2}\right)$	$\frac{s^2}{S_w}\left(\frac{2Q''_{23}}{k}-\frac{2Q'_{21}}{k^2}\right)$	$\frac{s^2}{S_w}\left(\frac{2Q''_{33}}{k}-\frac{2Q'_{31}}{k^2}\right)$	$\frac{s^2}{S_w}\left(\frac{2Q''_{i3}}{k}-\frac{2Q'_{i1}}{k^2}\right)$
$\dot{r}$	$-\frac{s^2}{S_w}\left(\frac{2Q'_{13}}{k^2}+\frac{2Q''_{11}}{k^3}\right)$	$-\frac{s^2}{S_w}\left(\frac{2Q'_{23}}{k^2}+\frac{2Q''_{21}}{k^3}\right)$	$-\frac{s^2}{S_w}\left(\frac{2Q'_{33}}{k^2}+\frac{2Q''_{31}}{k^3}\right)$	$-\frac{s^2}{S_w}\left(\frac{2Q'_{i3}}{k^2}+\frac{2Q''_{i1}}{k^3}\right)$
ξ_j	$\frac{s^2}{S_w}Q'_{1j}$	$\frac{s^2}{S_w}Q'_{2j}$	$\frac{s^2}{S_w}Q'_{3j}$	$\frac{s^2}{S_w}Q'_{ij}$
$\dot{\xi}_j$	$\frac{s^2}{S_w}\frac{Q''_{1j}}{k}$	$\frac{s^2}{S_w}\frac{Q''_{2j}}{k}$	$\frac{s^2}{S_w}\frac{Q''_{3j}}{k}$	$\frac{s^2}{S_w}\frac{Q''_{ij}}{k}$
δ	$\frac{s^2}{S_w}Q'_{1\delta}$	$\frac{s^2}{S_w}Q'_{2\delta}$	$\frac{s^2}{S_w}Q'_{3\delta}$	$\frac{s^2}{S_w}Q'_{i\delta}$
$\dot{\delta}$	$\frac{s^2}{S_w}\frac{Q''_{1\delta}}{k}$	$\frac{s^2}{S_w}\frac{Q''_{2\delta}}{k}$	$\frac{s^2}{S_w}\frac{Q''_{3\delta}}{k}$	$\frac{s^2}{S_w}\frac{Q''_{i\delta}}{k}$
α_g	$\frac{s^2}{S_w}Q'_{1\alpha_g}$	$\frac{s^2}{S_w}Q'_{2\alpha_g}$	$\frac{s^2}{S_w}Q'_{3\alpha_g}$	$\frac{s^2}{S_w}Q'_{i\alpha_g}$
$\dot{\alpha}_g$	$\frac{s^2}{S_w}\frac{Q''_{1\alpha_g}}{k}$	$\frac{s^2}{S_w}\frac{Q''_{2\alpha_g}}{k}$	$\frac{s^2}{S_w}\frac{Q''_{3\alpha_g}}{k}$	$\frac{s^2}{S_w}\frac{Q''_{i\alpha_g}}{k}$
β_g	$\frac{s^2}{S_w}Q'_{1\beta_g}$	$\frac{s^2}{S_w}Q'_{2\beta_g}$	$\frac{s^2}{S_w}Q'_{3\beta_g}$	$\frac{s^2}{S_w}Q'_{i\beta_g}$
$\dot{\beta}_g$	$\frac{s^2}{S_w}\frac{Q''_{1\beta_g}}{k}$	$\frac{s^2}{S_w}\frac{Q''_{2\beta_g}}{k}$	$\frac{s^2}{S_w}\frac{Q''_{3\beta_g}}{k}$	$\frac{s^2}{S_w}\frac{Q''_{i\beta_g}}{k}$

Subscripts of Q_{mn} indicate the mode shape:

1 = horizontal translation, 2 = rolling motion, 3 = yawing motion,
i,j = structural vibration, δ = control surface deflection,
α_g, β_g = gust